Acoustic anomalies in the phase transition vicinity in the weak ferroelectric $Li_2Ge_7O_{15}$

1995 J. Phys.: Condens. Matter 7 4283

(http://iopscience.iop.org/0953-8984/7/22/011)

J. Phys.: Condens. Matter 7 (1995) 4283–4298. Printed in the UK

Acoustic anomalies in the phase transition vicinity in the weak ferroelectric $Li_2Ge_7O_{15}$

I G Siny†, G O Andrianov†, A I Fedoseev†, V V Lemanov† and M D Volnyansky‡

† A F Ioffe Physical Technical Institute, RAC, St Petersburg 194021, Russia
‡ Dnepropetrovsk State University, Dnepropetrovsk, Russia

Received 30 August 1994, in final form 20 February 1995

Abstract. The behaviour of the sound velocity and damping in the phase transition vicinity in the weak ferroelectric $Li_2Ge_7O_{15}$ has been investigated by the ultrasonic technique (30–150 MHz) and by Brillouin scattering (about 40 GHz). A large critical contribution to the acoustic anomalies has been found in the paraelectric phase. Analysis of the sound velocity and damping dispersion revealed the relaxation parts of anomalies under conditions when the critical parts are large. The Landau theory is used to interpret the results obtained. Some coefficients in the thermodynamic potential expansion are determined. Increasing suppression of the relaxation anomalies by the depolarizing field as $T \to T_c$ is considered for both the sound velocity and the damping of longitudinal phonons with the wavevector along the polar axis. This is a specific feature of weak ferroelectrics.

1. Introduction

A ferroelectric phase transition in crystals of $Li_2Ge_7O_{15}$ (LGO) occurs within the orthorhombic crystal system from D_{2h}^{14} to C_{2v}^{5} [1–3]. A well defined soft mode in IR absorption [4] gives sufficient evidence of a phase transition without a change in the unit cell. A weak oscillator of the soft mode in the IR spectra [4] and almost no LO–TO splitting for soft-mode components in the Raman spectra [5] indicate a small value of the effective charge of the soft mode in LGO. In accordance with this substantial property, LGO possesses an extremely low Curie–Weiss constant C which is only about 2–4 K in the paraelectric phase [6–9].

The LGO crystals, therefore, afford us the opportunity of studying acoustic anomalies at the ferroelectric phase transition induced probably by a polar soft mode which is the weakest recorded. As the spontaneous polarization in LGO appears along the twofold axis, this crystal can be formally classified as a uniaxial ferroelectric but the depolarizing field effect is expected to be minimal because of the smallness of the soft-mode effective charge. In this case the order parameter fluctuations cannot be suppressed either; so we may expect some critical contribution to the acoustic anomalies near T_c due to fluctuations. Although some results of the ultrasonic measurements in LGO have been published [1, 7] and also a Brillouin study [10] of the behaviour of acoustic phonons with the wavevector $q \parallel b \perp P_s$, detailed analysis of acoustic anomalies in the vicinity of T_c has not been discussed yet. Also the influence of the macroscopic depolarization field has not been considered nor have the critical contributions been revealed. Some attempts to advance understanding in this direction were undertaken only in our preliminary publications [11, 12], which showed the importance of the dispersion effects in LGO in addition to the unusual features mentioned

0953-8984/95/224283+16$19.50

above. In the present paper we pay very full attention to the analysis of the sound velocity and damping anomalies near T_c in LGO mainly by studying their behaviour in a wide temperature interval and in a wide frequency range (from ultrasonic methods up to Brillouin scattering).

2. Experimental procedure and results

The LGO crystals belong to the orthorhombic system, but the ratio of the orthorhombic cell parameters $b \simeq \sqrt{3}c$ is close to that of a hexagonal structure with a sixfold axis along a. These structural relations show that the structure of the paraelectric phase can be created by a small distortion of some hexagonal parent phase. In other words, the room-temperature structure is simultaneously both a paraelectric phase with respect to the low-temperature ferroelectric phase transition and a ferroelastic phase with respect to another high-temperature phase transition. This point of view is evidenced by ferroelastic domains in some samples of LGO [13]. Our samples of LGO were found to be single-domain ferroelastic in the paraelectric phase. The spontaneous polarization in LGO occurs along the twofold axis which is the c direction in the unit cell: $c \parallel c_2$ [13]. So, we used the coordinate system with axes 1, 2 and 3 along the a, b and c edges, respectively, of the orthorhombic cell.

One sample of good optical quality was used for both ultrasonic and hypersonic measurements. The sample which has the form of a rectangular parallelepiped, 10 mm × 10 mm × 10 mm in size, was placed in an optical cell filled with glycerine for index matching, for precise stabilization of temperature and for minimization of temperature gradients in the course of measurements both from point to point and continuously; the latter was used for $\alpha(T)$. The optical cell with a sample was inserted in a cryostat into a stream of cold nitrogen vapour. In the region of the phase transition the temperature was stable to within 0.01 K. At continuous measurements the rate of temperature change was not more than 5×10^{-2} K min^{-1}.

Measurements of the sound velocities at ultrasonic frequencies of 30, 90 and 150 MHz were carried out with the usual pulse-echo method. The error in the determination of the absolute value of velocities did not exceed 10^{-2}, and it was no more than 10^{-3} in measurements of the relative changes in velocities during the temperature runs. The absolute values of elastic wave damping were determined by measuring the exponential drop in the echo-impulse amplitudes at room temperature. The temperature dependence of damping was obtained by automatic recording of the ultrasonic impulse amplitudes.

The Brillouin scattering spectra by longitudinal acoustic phonons were excited with an argon laser operating in a single mode at a wavelength λ of 488 nm. The scattered light was analysed with a three-pass Fabry–Pérot interferometer (Burleigh) with a DAS-1 system. We used a backward geometry in order to study the acoustic phonons with the largest wavevectors that were achievable in this method. In the course of experiments the Brillouin component shifts $\Delta\nu$ and their half-widths $\delta\nu$ were measured at every fixed temperature. The hypersonic velocity was calculated from the shifts of the Brillouin components relative to a laser line ν_0 by the well known formula

$$V = (\Delta\nu/\nu_0)(c/2n) = (\lambda/2n)\Delta\nu \tag{1}$$

where c is the speed of light in vacuum and for our 180° geometry one can use for the incident and the scattered light the same refractive index $n_1 = 1.743 \pm 0.005$ measured in our work at room temperature for the above-mentioned wavelength. The LGO crystal is

optically biaxial. However, our measurements and data in [14] showed that the birefringence is sufficiently small that the use of one value of the refractive index is justified in the limit of our accuracy. In calculating $V(T)$ we neglected the change in $n(T)$. However, the relative accuracy in measuring the hypersonic velocities was no more than $\pm 10^{-2}$. It is found that the velocity of hypersonic waves in the temperature region far from T_c exceeds the value obtained from ultrasonic measurement. The difference averages no more than 6%. Note that a similar tendency is found for Brillouin scattering data from [10] (see footnotes to tables 1 and 2 later) where Arai *et al*, who did not have the true value of the refractive index, used $n = 1.834$ to fit the ultrasonic and Brillouin data far from T_c. We believe that such a discrepancy is connected with the dispersion of the sound velocity for the frequencies lying in between the above-mentioned ultrasonic and hypersonic values. This requires some additional study. In order to succeed in using such a dispersion dependence of the sound velocity not connected with the phase transition we shall analyse only the relative change $V(T)/V^0$ in velocities for both ultrasonic and hypersonic measurements. Here $V(T)$ is the experimental value obtained for the velocity in the region of the phase transition and V^0 the expected value at $T = T_c$ in the absence of any phase transition. This value V^0 is calculated by extrapolation of the Brillouin shift behaviour from higher temperatures, as shown in figure 1. To increase the reliability in determining V^0 we measured the Brillouin component shifts in a wide temperature range above T_c. The value of $\Delta\nu(T)$ (as well as the value of $V(T)$ according to equation (1)) is almost unchanged in the large region 400 K < T < 600 K in the case of phonons with $q \parallel b$. In the other two cases, $q \parallel a$ and $q \parallel c$, the analogous analysis in the paraelectric phase gives a slow increase in $V(T)$ on cooling. We confined ourselves only to measurements of the Brillouin scattering. The ultrasonic value of V^0 is obtained by fitting the ultrasonic relative velocity to the hypersonic velocity at $T = T_c + 10$ K.

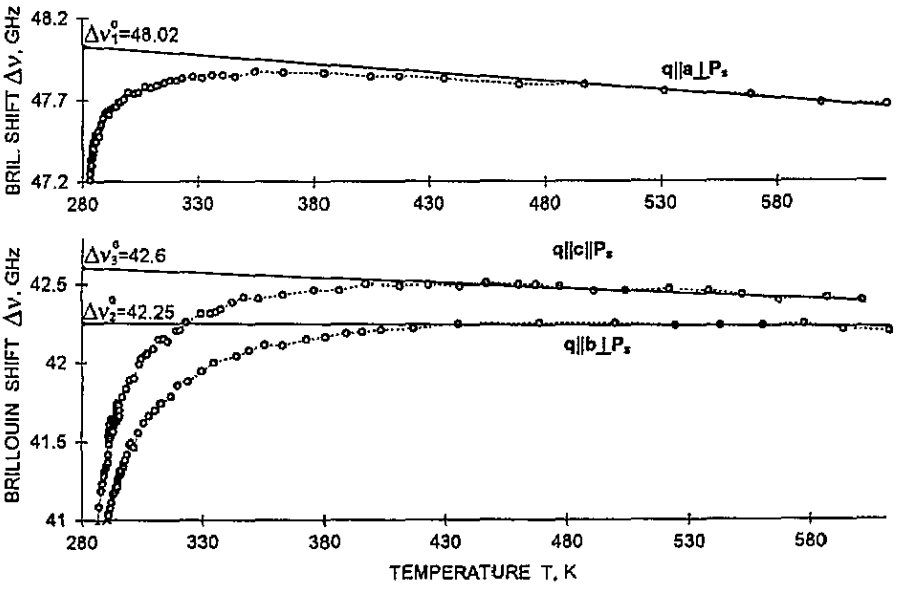

Figure 1. The temperature dependence of the Brillouin shift for the longitudinal phonons in the paraelectric phase: ——, extrapolated from high temperatures to estimate the values of $\Delta\nu_k^0$ (and V_k^0, respectively) ($k = 1, 2, 3$) at $T - T_c$.

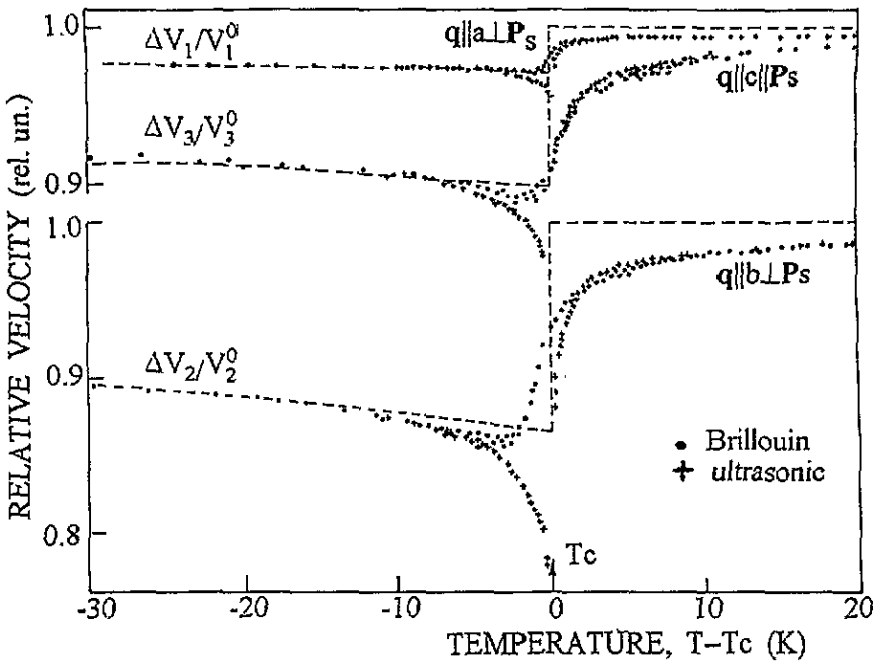

Figure 2. Relative change in sound velocity for longitudinal acoustic phonons with wavevector along the a, b and c directions in the orthorhombic unit cell: ●, Brillouin scattering measurements; +, ultrasonic data; – – –, behaviour of the relaxation part which is expected from the best fits of equation (7).

Figure 2 shows that the behaviours of the relative velocities for longitudinal acoustic phonons with wavevector q along the a, b and c directions at the ultrasonic frequencies and in Brillouin scattering were found to be undoubtedly different only in the phase transition region about $T_c \pm 10$ K. This is connected with dispersion effects in the vicinity of T_c. Besides a step-like anomaly of the sound velocity at $T = T_c$ in a wide temperature range of the paraelectric phase we observe a significant critical contribution in the velocity anomaly. A careful examination of this critical part, which we believe is connected with fluctuations of the polarization, will be given in a subsequent paper. It should be noted also that there is a noticeable temperature dependence of $V(T)/V^0$ in the ferroelectric phase connected with both the critical contribution and the closeness to the tricritical point phase transition.

Correspondingly the hypersonic damping is given by

$$\alpha\ (\mathrm{cm}^{-1}) = (2\pi n/\lambda)(\delta\nu/\Delta\nu). \tag{2}$$

Figure 3 shows the damping of these phonons in the case $q \parallel b \perp P_s$. We failed to make continuous measurements through the phase transition region at the ultrasonic frequencies owing to heavy damping in the vicinity of T_c. The gap is about 0.5 K at 30 MHz and about 2 K at 150 MHz. However, the Brillouin scattering allowed us to study the transition region although the Brillouin component width increased significantly in the vicinity of T_c up to $\delta\nu \simeq 0.15\Delta\nu$ owing to heavy damping. The error in determining the damping increased also. Nevertheless, we observed the double-peak structure of the damping maximum in hypersonic measurements. After careful analysis in [15] we revealed a relaxation part, the origin of which was confirmed by fitting equation (7) considered below. In accordance with the

relaxation origin, the peak location appears to be shifted from T_c to the ferroelectric phase. The remaining damping has a maximum value centred at T_c and represents a fluctuation contribution.

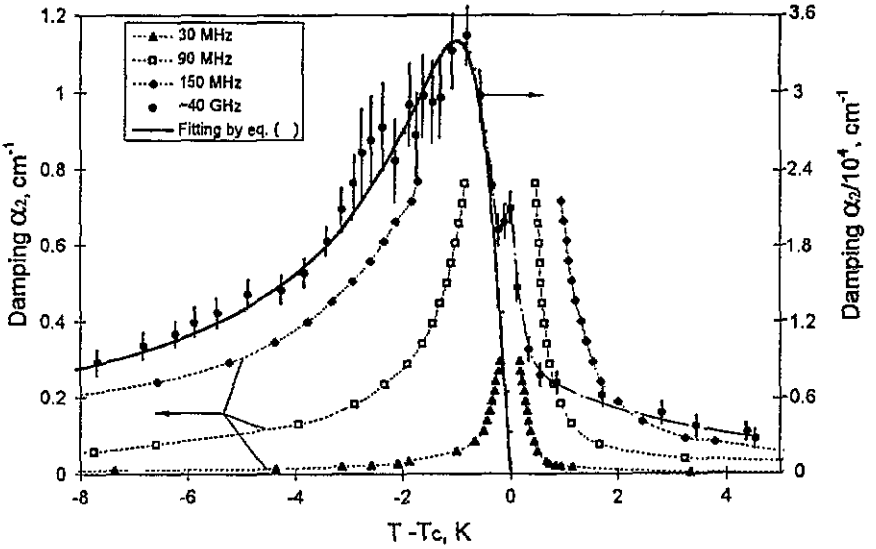

Figure 3. Damping maxima in the vicinity of T_c versus temperature for ultrasonic and hypersonic longitudinal phonons with $q \parallel b \perp P_s$: ----, — · —, guides to the eye.

Our data obtained for velocities agree well with other published results [1, 7, 10]. The elastic constants for LGO are shown in table 1. To calculate our data from the velocities measured by both the ultrasonic method and Brillouin scattering we used the density $\rho = 4.226 \times 10^3$ kg m^{-3} [2].

Table 1. Elastic moduli C_{ii}, $i = 1, 2, 3$, calculated from velocites of the longitudinal phonons with the wavevector along the a, b and c directions. $T = 293$ K.

	C_{11} (10^{10} N m^{-2})	C_{22} (10^{10} N m^{-2})	C_{33} (10^{10} N m^{-2})	Reference
Ultrasonic measurements	19.23	14.20	14.72	[1]
	16.51	12.86	13.23	[7]
	17.83 ± 0.17	12.76 ± 0.12	13.44 ± 0.13	This work
Brillouin scattering measurements	18.85 ± 0.18	14.02 ± 0.14	14.34 ± 0.14	This work
		12.85[a]		[10]

[a]The refractive index was chosen from the condition to provide the same sound velocity for both ultrasonic and hypersonic waves. The same data from [10] give $C_{22} = 14.1 \times 10^{10}$ N m^{-2} if another refractive index obtained in the present work is used.

Besides longitudinal phonons we also studied by the ultrasonic method transverse acoustic waves with wavevectors along a, b and c. The temperature dependences of velocity are shown in figure 4. As can be seen, no anomalies were found in the vicinity of T_c within the accuracy limit of our experiments. We compare our data for corresponding elastic constants with some other published data in table 2.

Table 2. Elastic moduli C_{kk}, $k = 4, 5, 6$, obtained from ultrasonic measurements. $T = 293$ K.

C_{44} (10^{10} N m^{-2})	C_{55} (10^{10} N m^{-2})	C_{66} (10^{10} N m^{-2})	Reference
4.46	3.41	—	[7]
$(3.87 \pm 0.03)^a$	3.46 ± 0.03	3.12 ± 0.03	This work

[a]For comparison, the Brillouin shift from [10] and the refractive index from the present work give $C_{44} = 4.25 \times 10^{10}$ N m^{-2}. See the footnote to table 1.

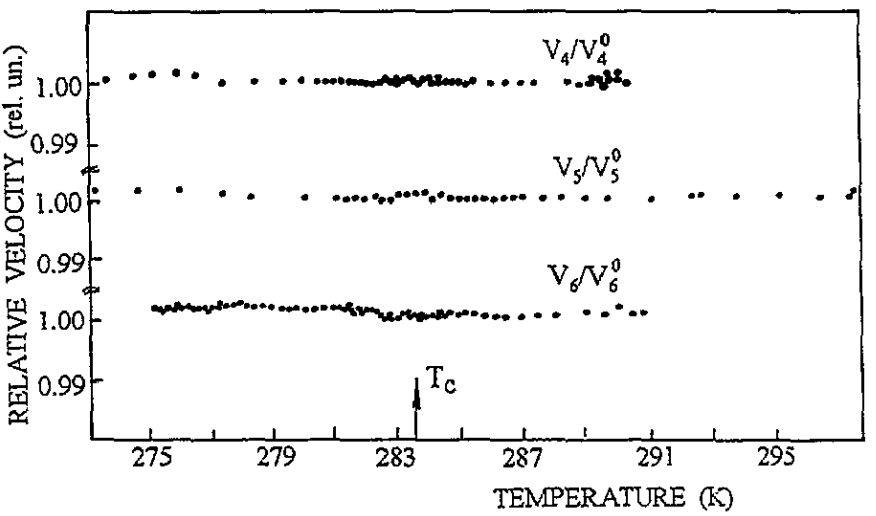

Figure 4. The temperature dependence of relative velocities for the transverse acoustic waves in the vicinity of T_c. The data are obtained by the ultrasonic method.

3. Analysis and discussion

3.1. Thermodynamic potential and elastic anomalies

The velocity and damping behaviour obtained from our experimental data for LGO can be interpreted in the framework of the phenomenological Landau theory, which was considered in detail for weak ferroelectrics in [16]. Taking into account the change in symmetry at the phase transition let us write the potential of interaction between the polarization P and the strains u_k in the form

$$\Phi_{\text{inter}}(P, u, T) = g_{3k} P^2 u_k + h_{3k} P^2 u_k^2. \tag{3}$$

Therefore using the theoretical results of [16, 17] the following expression can be derived for complex addition to elasticity moduli of longitudinal phonons below T_c:

$$\Delta C_{kk}^* = -\frac{4 g_{3k} P_0^2}{\chi^{-1}} \frac{1}{1 + \Omega^2 \tau^2} + 2 h_{3k} P_0^2 \tag{4}$$

where an expression for the reciprocal susceptibility $\chi^{-1} = (\partial^2 \Phi / \partial P^2)_0$ appears to be essentially different for longitudinal phonons with the wavevector perpendicular to and along the spontaneous polarization P_s because of the macroscopic depolarizing field in the

last case. This is well known for the usual uniaxial ferroelectrics [18] and for weak uniaxial ferroelectrics [16]. We have for weak ferroelectrics

$$\chi^{-1} = \begin{cases} \alpha + 3\beta_1 P_0^2 + 5\gamma P_0^4 & \text{if } q \perp P_s \quad (5) \\ \alpha + 3\beta_1 P_0^2 + 5\gamma P_0^4 + 4\pi/\varepsilon^* & \text{if } q \parallel P_s \quad (6) \end{cases}$$

where P_0 is the equilibrium value and ε^* is the background dielectric constant. $\alpha = \lambda(T - T_c)$, and β and γ are the usual coefficients of Landau expansion for the thermodynamic potential in powers of P. $\beta_1 = \beta - 2g_{3k}/C_{ik}^0$, where the background elastic constants C_{ik}^0 are assumed to vary linearly with temperature owing to thermal expansion in the same manner as we defined for V^0 above.

If a phase transition belongs to the second order ($\gamma \equiv 0$) and if the dipole–dipole interaction does not give rise to a depolarizing field, the first term in equation (3) causes both a step-like anomaly in the sound velocity at T_c and an asymmetrical Landau–Khalatnikov maximum in damping. Thus, as the sound velocity has a strong temperature dependence in the ferroelectric phase (figure 2), we take into account the term with $\gamma \neq 0$ and the second term in equation (3). The possible contribution of the last term to the anomaly of longitudinal waves will be discussed below. As to transverse waves, this term does not give any perceptible contribution because the temperature dependences of the velocities do not show any appreciable change at T_c (figure 4). So, the coefficients h_{3k} ($k = 4, 5, 6$) in LGO are negligibly small.

3.2. Analysis of the 'usual' anomalies for phonons with $q \perp P_s$

To begin with, let us consider the geometry $q \perp P_s$. A change in the behaviour of the sound velocity and damping for the longitudinal elastic waves propagating along the crystallographic axes a and b in the vicinity of the phase transition follows directly from equation (4):

$$\frac{\Delta V_k}{V_k^0} = -\frac{g_{3k}^2}{\beta\rho V_k^2}\frac{1}{[1 + (T_c - T)/\Delta T]^{1/2}}\frac{1}{1 + \Omega^2\tau^2} + \frac{h_{3k}\beta}{2\gamma\rho V_k^2}\left[\left(1 + \frac{T_c - T}{\Delta T}\right)^{1/2} - 1\right] \quad (7)$$

$$\Delta\alpha_k = -\frac{g_{3k}^2}{\beta\rho V_k^3}\frac{1}{[1 + (T_c - T)/\Delta T]^{1/2}}\frac{\Omega^2\tau}{1 + \Omega^2\tau^2} \quad (8)$$

where ΔT characterizes the proximity of a phase transition to a tricritical point, $\Delta T = \beta^2/4\lambda\gamma$ and $k = 1, 2$.

To eliminate the influence of the dispersion fraction $(1 + \Omega^2\tau^2)^{-1}$ in equation (7), let us take advantage of ultrasonic measurements satisfying the condition $\Omega\tau \ll 1$ and evaluate the step-like anomaly in the sound velocity at $T = T_c$. As a first approach which is used very often we shall ignore the contribution of fluctuations, defects or other effects which cause the strong temperature dependence of sound velocities in the paraelectric phase near T_c (figure 1). The step-like anomaly $\Delta V_2/V_2^0 = 0.18$ is obtained from the best fit of equation (7) to the experimental points in the narrow temperature interval $T_c - T < 9$ K (the chain curve in figure 5). The fit of ultrasonic data to this calculation appears to be unsatisfactory especially in a wider temperature region, and the small value of $\Delta T = 9$ K given by fitting is not confirmed by the temperature dependence of ultrasonic damping (the broken curve in figure 6). Experimental data for three ultrasonic frequencies are well fitted by a hyperbola $\alpha/\Omega^2 \sim \tau \sim (T_c - T)^{-1}$ with $\tau = \tau_0(T_c - T)^{-1} = 4.3 \times 10^{-12}(T_c - T)^{-1}$ s

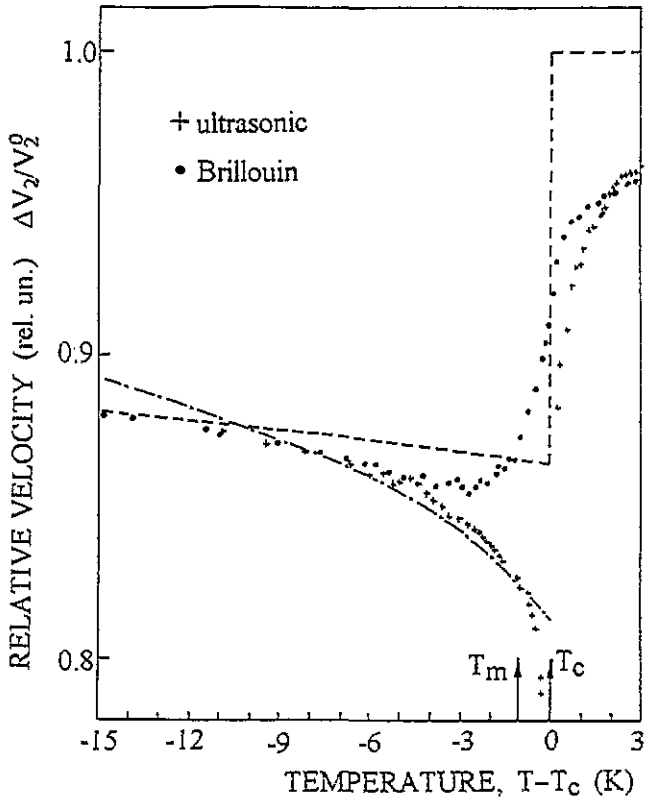

Figure 5. The sound velocity anomalies in the vicinity of T_c for longitudinal phonons with the wavevector $q \parallel b \perp P_s$: +, behaviour at 30 MHz; — · —, rough attempt at calculation when an acceptable fit of equation (7) is seen not far away from T_c at $T_c - T < 9$ K; – – –, same curve as in figure 2 in a wider temperature region showing the final result of the best fit of equation (7) when the step-like anomaly for the sound velocity at $T = T_c$ is obtained from independent measurements.

as shown by the solid curve through the experimental points in figure 6. The latter result indicates the phase transition to be far from the tricritical point. Note that the step-like change $\Delta V_2/V_2^0 = 0.18$ is considerably larger than values estimated by other methods.

Let us consider these methods. The hypersonic damping reaches its peak value at $T = T_m$ simultaneously with the fulfilment of the condition $\Omega\tau = 1$. This temperature point corresponds to half the velocity step as follows from equation (7). The difference between the ultrasonic and hypersonic velocity values at this point equals half the step also. A whole velocity step can be easily restored. A gap in the low-frequency ultrasonic data for velocity in the vicinity of T_c gives another value for the velocity step. One more value is given by analysing the hypersonic damping at $T = T_m$. One should note that such simple calculations become difficult in the case of LGO owing to large critical contributions. If the critical contribution growing in the paraelectric phase is well seen and can be analysed, the law for its decrease in the ferroelectric phase is not known precisely. Another uncertainty in determining the low point for the velocity step appears owing to the dispersion of the critical contribution. However, if the dispersion of the relaxation contribution, which is determined with precision by the fraction $(1 + \Omega^2\tau^2)^{-1}$ in equation (7), is analysed not at

$T = T_m$ but at some distance deeper in the ferroelectric phase, one can avoid the faults mentioned above. The critical contribution dispersion in the paraelectric phase in LGO fades away at $T \geqslant T_c + 2$ K. If we take a mirror temperature point at the same distance away from T_c in the ferroelectric phase, namely $T = T_c - 2$ K, we obtain $\Omega\tau = 0.5$ and find that the difference between the hypersonic and ultrasonic velocities equals 0.2 of a whole velocity step at $T = T_c$, which is now easily restored from experimental data.

Our analysis has given an average value of $\Delta V_2/V_2^0 = 0.135$ for the longitudinal phonons with $q \parallel b \perp P_s$ (figure 5).

3.3. Proximity to a tricritical point

In this section we have to fit the behaviour of $V_2(T)$ in the ferroelectric phase with good precision in order to find a deviation from that for the longitudinal phonons with $q \parallel c \parallel P_s$ in the next section. We have determined the velocity step of $\Delta V_2/V_2^0$ (or $g_{32}^2/\beta\rho V_2^2$ in equation (7)) from independent measurements. This provides a good starting point, Two other values, ΔT and h_{32}, in equation (7) remain as adjustment parameters. The limiting case with $\gamma = 0$ (or $1/\Delta T = 0$ in equation (7)) and $h_{32} = 0$ in equation (3) does not agree with a non-linear change in $V_2(T)$ in the ferroelectric phase. If we take only $h_{32} \neq 0$, the last term in equation (7) has a linear temperature dependence and because of this an increasing discrepancy between experimental data and calculations is expected at temperatures $T_c - T \geqslant 40$ K. The best fitting in a wide temperature interval (figures 2 and 5) was obtained with $\Delta T = 45$ K and a small coefficient h_{32} so that the contribution of the last term in equation (7) to $V_2(T)$ even far from T_c at $T_c - T \simeq 100$ K was about 1%.

So, it would seem that the strong temperature dependence of $V_2(T)$ in the vicinity of the transition point shows the phase transition which is close to a tricritical point. We started from $\Delta T = 9$ K and obtained some contradiction between our results. More careful and concerted analysis indicates that the phase transition in LGO is even farther away from the tricritical point. On the whole, our conclusion agrees with other published data. The ratio of the Curie–Weiss constants above and below T_c in LGO was found to be mainly about 2 [6,7,9]. The value $\Delta T = 15$ K was obtained from specific-heat measurements for LGO [19]. Note that there are some contradictions in the values of ΔT in the series of papers in [19–21]. The values of λ, β and γ taken from these studies to determine ΔT give different values, e.g. $\Delta T \simeq 3$ K and even $\Delta T \simeq 350$ K, and there are other contradictions.

The values of g_{3k}^2/β obtained for the present case, $q \parallel b$, and for phonons with $q \parallel a$ from a similar consideration are given in table 3.

Table 3. Electrostrictive and piezoelectric coefficients determined from the sound velocity steps at $T = T_c$ and calculated at $T_c - T = 7.5$ K.

		$T = T_c$			$T_c - T = 7.5$ K	
Phonon wavevector	k	$2g_{3k}^2/\beta$ (10^{10} N m^{-2})	g_{3k} (10^{14} V m C^{-1})	Q_{3k} (m^4 C^{-2})	q_{3k} (m^2 C)	d_{3k} (10^{-12} C N^{-1})
$q \parallel a$	1	0.7	0.7	280	0.1	0.3
$q \parallel b$	2	2.9	1.4	1110	0.4	1.2
$q \parallel c$	3	2.4	1.3	970	0.4	1.0

3.4. Analysis of the partial suppression of anomalies for phonons with $q \parallel P_s$

Now let us consider the longitudinal acoustic phonons with $q \parallel c \parallel P_s$. To obtain working formulae for calculating the behaviour of the relaxation parts in sound velocity and damping such as equations (7) and (8) in the previous case, we should take a modified expression (6) for χ^{-1}. We are interested in the partial suppression of the relaxation anomalies in the so-called dipole region which is very narrow for LGO owing to the smallness of the depolarizing field. Therefore we need our formulae to be valid near T_c in a narrow region about $T_c - T_m = 1$ K; so we can neglect both the contribution of the term with h_{33} in equation (3) and the temperature dependence of $V_3(T)$ in the narrow region by putting $\gamma = 0$. Instead of equations (7) and (8) we now obtain

$$\frac{\Delta V_3}{V_3^0} = -\frac{g_{33}^2}{\beta\rho V_3^2}\frac{1}{1+2\pi/\varepsilon^*\lambda(T_c-T)}\frac{1}{1+\Omega^2\tau^2} \tag{9}$$

$$\Delta\alpha_3 = -\frac{g_{33}^2}{\beta\rho V_3^3}\frac{1}{1+2\pi/\varepsilon^*\lambda(T_c-T)}\frac{\Omega^2\tau}{1+\Omega^2\tau^2} \tag{10}$$

where $\Delta V_3/V_3^0 = g_{33}^2/\beta\rho V_3^2$ corresponds to a step-like anomaly in the absence of the depolarizing field. This value shown in table 3 was obtained by the extrapolation of V_3^0 from above (figure 1) and by fitting $V_3(T)$ from below according to equation (7) with $\Delta T = 45$ K found above. We supposed that the term with h_{33} gave a small contribution analogously to that in the situation with h_{32} considered above. The correctness of this suggestion is obvious because the b and c directions in LGO become equivalent in the hexagonal parent phase, and the difference between the behaviours of $V_2(T)$ and $V_3(T)$ in the paraelectric phase does not exceed 0.5% (figure 1). It is therefore not surprising that the changes in $\Delta V/V^0$ at T_c are found to be nearly the same in these two cases (table 3).

The calculated step-like anomaly of $\Delta V_3/V_3^0$ in the vicinity of the transition in LGO is shown in figure 7(a). The broken curve in figure 7(a) shows the partial suppression of the 'free' step-like anomaly. The broken curve follows equation (9) without the dispersion fraction, i.e. on the supposition that $\Omega\tau \ll 1$. The step-like anomaly for the sound velocity appears to be stretched in the same manner as under the influence of the dispersion. In turn, the dispersion provides additional modification of the anomaly. Moreover, a special relaxation time should be taken into account for phonons with $q \parallel P_s$. According to definition, the relaxation time is determined through the polarization viscosity μ and the susceptibility χ, namely $\tau = \mu\chi$, where χ is given by a modified equation (6) for phonons with $q \parallel P_s$. Simplifying the situation in the vicinity of T_c by putting $\gamma = 0$ as above for equations (9) and (10), we have for $\tau = \tau_\parallel$

$$\tau_\parallel = \mu\chi_\parallel \simeq \mu/[2\lambda(T_c - T) + 4\pi/\varepsilon^*] = \tau_0/[(T_c - T) + 2\pi/\varepsilon^*\lambda] \tag{11}$$

where $\tau_0 = 4.3 \times 10^{-12}$ K s was determined above from experimental data for the damping of phonons with $q \perp P_s$ (figure 6). In figure 7(b) we show a dispersion 'stretching' of the step-like anomaly $\Delta V_3/V_3^0$ for two relaxation times: $\tau_\parallel$ from equation (11) (dotted curve) and $\tau_\perp = \mu\chi_\perp$ with $\chi_\perp$ from equation (5) (chain curve). As one can see, the condition $\Omega\tau_\parallel < \Omega\tau_\perp$ is characteristic of weak ferroelectrics. The difference is not so large for LGO (figure 7); however, the $\Omega\tau_\parallel \to 1$ limit is not approached for Brillouin scattering in TSCC and the condition $\Omega\tau_\parallel < 1$ continues to be valid in the vicinity of T_c for phonons with $q \parallel P_s$ while the Landau–Khalatnikov maximum with $\Omega\tau_\perp = 1$ is achieved for phonons with $q \perp P_s$ [16].

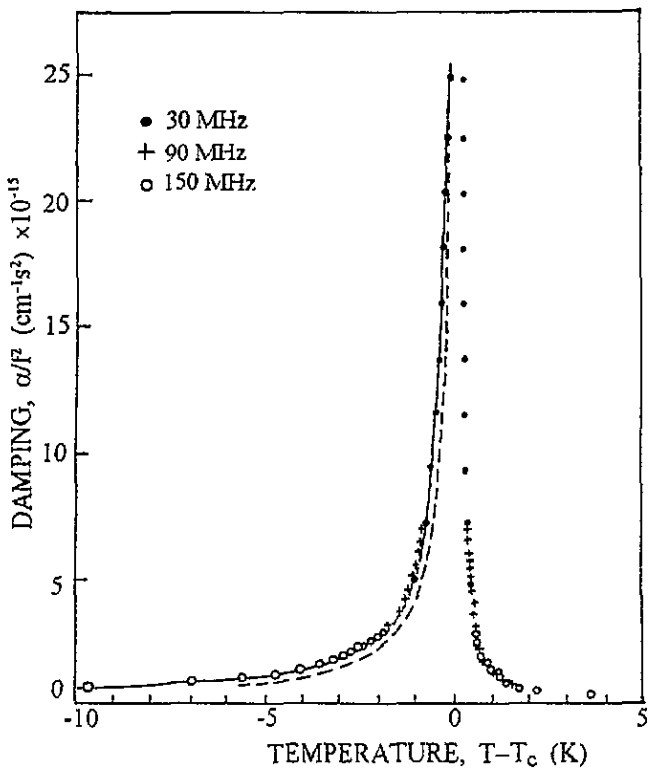

Figure 6. The anomalous damping divided by the square of frequency as a function of temperature in the vicinity of T_c: ——, curve through experimental points in the ferroelectric phase follows a hyperbolic dependence $\alpha/f^2 \sim (T_c - T)^{-1}$ that is valid for a second-order phase transition; – – –, expected behaviour if the phase transition is not so far from a tricritical point ($\Delta T = 9$ K) (this corresponds to the sound velocity anomaly shown by the chain curve in figure 5).

The difference between the 'initial' step for $\Delta V_3/V_3^0$ and the real behaviour modified by both a partial depolarizing suppression and dispersion is finally shown by a pair of curves in figure 7(*c*).

As one can see, the net effect 'stretches' an 'initial' anomaly very significantly in comparison with that under the influence of dispersion only. However, our calculation ignores critical contributions to the acoustic anomalies. It seems that, making a comparison of the revealed critical parts in the two cases of phonons with $\boldsymbol{q} \perp \boldsymbol{P}_s$ and $\boldsymbol{q} \parallel \boldsymbol{P}_s$ we can judge whether our manipulations with the relaxation parts are right or wrong. If the relaxation parts in these two cases, $\boldsymbol{q} \perp \boldsymbol{P}_s$ and $\boldsymbol{q} \parallel \boldsymbol{P}_s$, are different and follow different equations (7) and (9), respectively, the rest of the anomaly, which means the critical part, is expected to have the same temperature behaviour in both cases.

3.5. Comparison of sound velocity anomalies for phonons with $\boldsymbol{q} \perp \boldsymbol{P}_s$ and $\boldsymbol{q} \parallel \boldsymbol{P}_s$

Figure 8 shows the experimental data from Brillouin scattering for sound velocity anomalies in the vicinity of T_c in two geometries: $\boldsymbol{q} \perp \boldsymbol{P}_s$ (figure 8(*a*)) and $\boldsymbol{q} \parallel \boldsymbol{P}_s$ (figure 8(*b*)). The broken curves in both figures represent the behaviour without the critical parts which is expected from equations (7) and (9), respectively. The shaded areas bordered by dotted

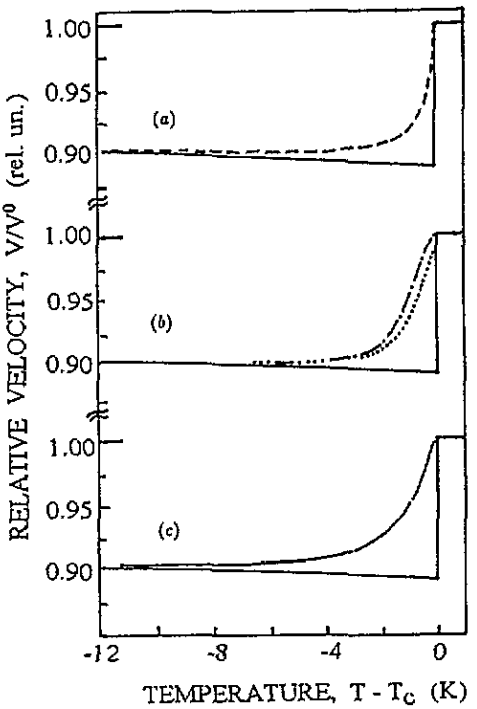

Figure 7. Modifications of the velocity step-like anomaly for longitudinal phonons with $q \parallel c \parallel P_s$ due to partial suppression (– – – in (*a*)), due to dispersion with the relaxation times $\tau_\perp$ (— · — in (*b*)) or $\tau_\parallel$ (· · · · · in (*b*)) and due to both of them simultaneously (the 'stretched' anomaly in (*c*)): ——, the initial calculated anomaly for $\Delta V_3/V_3^0$ shown in (*a*), (*b*) and (*c*).

curves in the ferroelectric phase give critical parts revealed as a difference between the experimental points and the latter calculations. So, the solid curves through experimental points are fits of equations (7) and (9) plus corresponding critical parts. In spite of the completely different analysis of relaxation parts in the two cases $q \perp P_s$ and $q \parallel P_s$, the residual critical parts in the ferroelectric phase in both cases are nearly the same as is well seen by comparison of figures 8(*a*) and 8(*b*). This proves that our approach is correct. This result also agrees with the similarity of critical parts in the paraelectric phase. Such a similarity follows from what we discussed above regarding the paraelectric phase that is a slightly distorted hexagonal parent phase from a symmetry point of view.

Our calculations show that the anomalous behaviour of some values determined by equations (9)–(11) is a function of λ. Analysing a partial suppression of both the sound velocity step and the Landau–Khalatnikov damping given by equations (9) and (10) together with a modified relaxation time $\tau_\parallel$ given by equation (11), we found an average value for the thermodynamic coefficient $\lambda \simeq 3.5 \times 10^{10}$ V m C^{-1} K^{-1}. This value obtained from acoustic anomalies agrees well with $\lambda = 2.46 \times 10^{10}$ V m C^{-1} K^{-1} appearing in the literature [8, 19–21]. The latter was found from dielectric measurements [7], namely from a Curie–Weiss law analysis. This value of $\lambda = 1/C\varepsilon_0$ corresponds probably to the highest value of the Curie–Weiss constant $C^+ = 4.6$ K [7] although other lower values are known for LGO, namely 3 K [9] and 2.05 K [6, 8]. So, the value of λ ranges between 2.5×10^{10} and 5.5×10^{10} V m C^{-1} K^{-1} even calculated by one method.

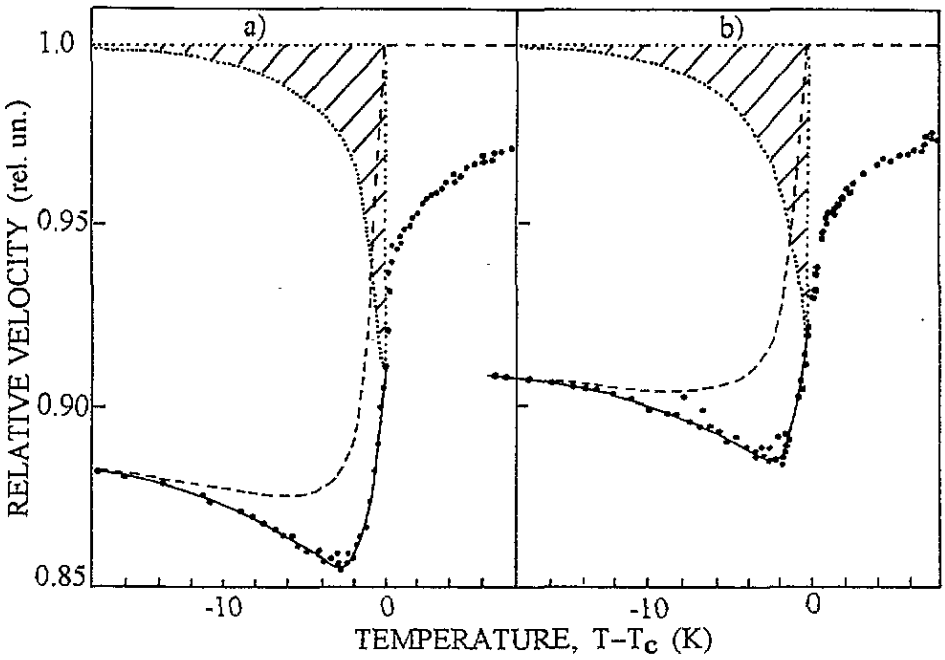

Figure 8. Comparison of sound velocity anomalies for longitudinal phonons with (*a*) $q \parallel b \perp P_s$ and (*b*) $q \parallel c \parallel P_s$: – – –, curves following equation (7) in (*a*) and equation (9) in (*b*). The two shaded areas represent corresponding critical parts revealed in the ferroelectric phase for comparison.

One should note that the Curie–Weiss law in LGO is fulfilled in a narrow temperature region in the vicinity of T_c, namely $T - T_c \leqslant 4$ K [17]. A significant critical contribution to the temperature dependence of $\varepsilon_c - \varepsilon^*$ is expected in LGO like that in TSCC [22]. The appearance of a critical part in the dielectric response is argued by direct analogy with the behaviour of acoustic anomalies also. If the critical part is sufficiently large and is not subtracted correctly before calculation, then the λ-value obtained does not correspond to the true thermodynamic coefficient in the Landau expansion which is valid beyond a critical region. Our calculation from equations (9)–(11) is based on analysis of the relaxation part; so it gives a true value for λ in LGO. Unfortunately, correction of all coefficients in the Landau expansion is needed in the vicinity of T_c where the contribution of fluctuation in LGO is very large. This problem seems to be rather complicated at present.

3.6. The expansion coefficients and electrostrictive constants in weak ferroelectrics

The existence of a soft mode in the Brillouin zone centre [4, 7] allows us to consider LGO as a displacive-type ferroelectric. Such crystals possess mostly a large Curie–Weiss constant: $C \simeq 10^5$ K [23]. Then the weak ferroelectrics of LGO type have, according to definition, the largest constants $\lambda \sim 1/C$ for ferroelectrics. The coefficient λ in LGO differs from that in an ordinary displacive ferroelectric by five orders of magnitude. The next coefficient β in the Landau expansion appears to be even more different from the common value because the spontaneous polarization in weak ferroelectrics is small in accordance with a small effective charge of the soft mode. It is easily seen in the case of the second-order phase transition

with $\gamma = 0$, when the resultant equilibrium value P_0 is given by

$$P_0^2 \sim \lambda(T_c - T)/\beta. \tag{12}$$

To determine β, we made use of some data on the shift of the Curie temperature in LGO under application of an external electric field [24]. We obtained $\beta = 1.4 \times 10^{18}$ V m^5 C^{-3} which is twice that in [24] because we used a slightly different formula [23, 25]. Evaluation of β from equation (12) with other P_s from [7] at $T_c - T = 7.5$ K gave $\beta = 4.6 \times 10^{18}$ V m^5 C^{-3}. However, we assume that equation (12) is not valid that far away from T_c in LGO owing to an unusual temperature dependence of P_s which even changes sign at $T = 178$ K [26]. Therefore, the first value of β obtained from the data in the vicinity of T_c seems to be the most reasonable. Note that measurements of the specific-heat anomaly near T_c in LGO give $\beta = 7 \times 10^{19}$ V m^5 C^{-3} [20]. So, we have found the coefficient β in LGO to be larger by seven to eight orders of magnitude than that in 'ordinary' ferroelectrics. This conclusion seems to be common to both LGO and TSCC considered previously [16] and is expected to be general for weak ferroelectrics. Anomalous values of the coefficients do not result from an accidental conjunction of parameters but are connected with the origin of the phase transition which is initiated by shorter-range forces than the Lorentz component of the dipole–dipole interaction.

If the value of β is large, the ordinary step-like sound velocity anomaly $\Delta V/V^0 \simeq 0.1$–0.2 at $T = T_c$ can occur only in crystals with the abnormal electrostrictive coefficients. In fact, while the value of $2g_{3k}^2/\beta$ for LGO is about four times that for $Pb_5Ge_3O_{11}$, the bare electrostrictive constant g_{32} in LGO exceeds g_{31} for $Pb_5Ge_3O_{11}$ [27] and g_{12} and g_{13} for $Sn_2P_2S_6$ [28] by five and six orders of magnitude, respectively. As shown in [29], the electrostrictive constants in weak ferroelectrics may differ considerably if they are determined by different methods. This is the reason why we compare here the electrostrictive constants for LGO, $Pb_5Ge_3O_{11}$ and $Sn_2P_2S_6$ which were obtained by the same method from the step-like anomalies of ultrasonic and hypersonic velocities at ferroelectric phase transitions in uniaxial ferroelectrics of displacive type. The value of g_{3k} ($k = 1, 2, 3$) for LGO obtained in the present work are shown in table 3.

The electrostrictive coefficients g_{3k} connect arising strains with P_s^2. It is easy to transfer from g_{3k} to the other electrostrictive coefficients Q_{3k} which determine the appearance of deformations: $g_{3k} = C_{kk}^P Q_{3k}$, where C_{kk}^P is the 'clamped' elastic modulus. The values obtained here for Q_{3k} for LGO (table 3) appear to be the largest among the published data for different ferroelectrics [30]. Note that these coefficients for LGO prove to be larger than those for both TGS and $BaTiO_3$ by two to three and by four to five orders of magnitude, respectively.

In the ferroelectric phase of LGO, one can transfer from the electrostrictive to the piezoelectric coefficients $q_{3k} = 2Q_{3k}P_s$ and then to the piezoelectric moduli $d_{3k} = 2Q_{3k}P_s(\varepsilon_3 - \varepsilon^*)\varepsilon_0$, which are mostly measured in experiments. As, in the expression above, $(\varepsilon_3 - \varepsilon^*) \sim (T_c - T)^{-1}$ in accordance with the Curie–Weiss law and $P_s \sim (T_c - T)^{1/2}$ according to equation (12), the corresponding moduli d_{3k} should increase at $T \to T_c$. In fact, the dynamic piezoelectric modulus d_{33} was found to increase ten times near T_c [6]. Therefore we calculated the piezoelectric coefficients from our data at some temperature shifted from T_c to the ferroelectric phase, namely at the point $T_c - T = 7.5$ K where the value of P_s is known [7]. One can believe that the Curie–Weiss law $\varepsilon_3 - \varepsilon^* = C^-/(T_c - T)$ is still valid at this distance from T_c for our purposes although a narrower region $T_c - T \leqslant 2$ K is shown for adherence to the law in some cases [7]. We find that the results of our calculation of d_{3k} (table 3) agree with the data obtained from independent measurements [31]: $d_{32} \simeq d_{31} \simeq 1$ pC N^{-1}.

4. Conclusion

The acoustic response of a ferroelectric crystal has been studied in the vicinity of the phase transition under special conditions which arise from the large critical contributions and from the macroscopic depolarizing field in the partial geometry $q \parallel P_s$. In the present paper we do not look for the origin of the critical contributions. To answer this question, the temperature dependence of contributions should be analysed first of all. A preliminary examination [12] showed the presence of fluctuation contributions although some contribution of defects is not excluded. Here we would like to emphasize that the LGO crystal is unique in some respects because the critical contributions to ultrasonic and hypersonic velocities increase obviously in the paraelectric phase at $T \to T_c$ from above and become comparable with the relaxation step-like anomalies expected from the Landau theory. We demonstrated that in such circumstances a comparative analysis of ultrasonic and hypersonic data allows us to reveal the relaxation contribution to the total anomaly. The behaviour of these contributions is well described by the Landau theory. Making a comparison between the theory and experimental data we calculated the piezoelectric moduli for LGO by successive performances in the chain $2g_{3k}^2/\beta \to g_{3k} \to Q_{3k} \to q_{3k} \to d_{3k}$. The latter result agrees with that from independent direct measurements [31]. In the case of longitudinal phonons with $q \parallel P_s$ we succeeded not only in revealing the residual relaxation anomalies but also in explaining the character of their suppression by the depolarizing field. This effect is specific to weak ferroelectrics which LGO is. This new approach allows us to determine the coefficient λ in an unusual way from acoustic measurements. This approach appears to be correct because there is reasonable agreement between our calculation and direct dielectric measurements.

Acknowledgment

The research described in this paper was made possible in part by grant N R5F000 from the International Science Foundation.

References

[1] Haussühl S, Wallrafen F, Recker K and Eckstein J 1980 *Z. Kristallogr.* **153** 329
[2] Völlenkle H, Wittmann A and Nowotny H 1970 *Monatsh. Chem.* **101** 46
[3] Terauchi H, Iida S, Nishihata Y, Wada M, Sawada A and Ishibashi Y 1983 *J. Phys. Soc. Japan* **52** 2312
[4] Volkov A A, Kozlov G V, Goncharov Y G, Wada M, Sawada A and Ishibashi Y 1985 *J. Phys. Soc. Japan* **54** 818
[5] Wada M, Sawada A and Ishibashi Y 1984 *J. Phys. Soc. Japan* **53** 3319
[6] Preu P and Haussühl S 1982 *Solid State Commun.* **41** 627
[7] Wada M and Ishibashi Y 1983 *J. Phys. Soc. Japan* **52** 193
[8] Volnyansky M D and Kidzin A Ju 1987 *Fiz. Tverd. Tela* **29** 213 (Engl. Transl. 1987 *Sov. Phys.–Solid State* **29** 119)
[9] Hookah M, Sawada A and Wada M 1989 *J. Phys. Soc. Japan* **58** 3793
[10] Arai M, Arima M, Sakai A, Wada M, Sawada A and Yagi T 1987 *J. Phys. Soc. Japan* **56** 3213
[11] Siny I G, Fedoseev A I and Volnyansky M D 1990 *Fiz. Tverd. Tela* **32** 353 (Engl. Transl. 1990 *Sov. Phys.–Solid State* **32** 202)
[12] Lemanov V V and Siny I G 1991 *Ferroelectrics* **117** 105
[13] Wada M, Sawada A and Ishibashi Y 1981 *J. Phys. Soc. Japan* **50** 1811
[14] Kaminsky W and Haussühl S *Ferroelectrics Lett.* **11** 63
[15] Siny I G, Fedoseev A I and Volnyansky M D 1990 *Fiz. Tverd. Tela* **32** 3130
[16] Smolensky G A, Siny I G, Tagantsev A K, Prokhorova S D, Mikvabiya V D and Windsch W 1985 *Zh. Eksp. Teor. Fiz.* **88** 1020 (Engl. Transl. 1985 *Sov. Phys.–JETP* **61** 599)

[17] Lemanov V V, Esayan S K and Shapel J P 1981 *Fiz. Tverd. Tela* **23** 262 (Engl. Transl. 1981 *Sov. Phys.–Solid State* **23**)
[18] Geguzina S Ya and Krivoglaz M A 1967 *Fiz. Tverd. Tela* **9** 3095
[19] Strukov B A, Kozhevnikov M Yu, Nizomov H A and Volnyansky M D 1991 *Fiz. Tverd. Tela* **33** 2962
[20] Strukov B A, Kozhevnikov M Yu, Sorokin E L and Volnyansky M D 1990 *Fiz. Tverd. Tela* **32** 2823
[21] Strukov B A, Kozhevnikov M Yu, Volnyansky M D and Nizomov H A 1991 *Kristallografiya* **36** 942
[22] Sandvold E and Courtens E 1983 *Phys. Rev.* B **27** 5660
[23] Lines M E and Glass A M 1977 *Principles and Applications of Ferroelectrics and Related Materials* (Oxford: Clarendon) p 736
[24] Volnyansky M D, Kudzin A Ju and Makarenko I I 1987 *Fiz. Tverd. Tela* **29** 3471 (Engl. Transl. 1987 *Sov. Phys.–Solid State* **29** 1991)
[25] Bornarel J and Schmidt V H 1981 *J. Phys. C: Solid State Phys.* **14** 2017
[26] Bush A A and Venevtsev Yu N 1986 *Fiz. Tverd. Tela* **28** 1970 (Engl. Transl. 1986 *Sov. Phys.–Solid State* **28** 1101)
[27] Avakyants L P, Glushkova T M, Kiselev D F and Molodtsov V V 1986 *Fiz. Tverd. Tela* **28** 749 (Engl. Transl. 1986 *Sov. Phys.–Solid State* **28** 417)
[28] Valyavichus V D 1981 *Thesis* Vilnius University
[29] Tagantsev A K, Siny I G and Prokhorova S D 1987 *Izv. Akad. Nauk. SSSR, Ser. Fiz.* **51** 2082 (Engl. Transl. 1987 *Bull. Acad. Sci. USSR* **51** 2082)
[30] *Landolt–Börnstein New Series* 1984 Group III, vol 18 (Berlin: Springer)
[31] Volnyansky M D and Kudzin A Ju 1987 *Fiz. Tverd. Tela* **29** 3123 (Engl. Transl. 1987 *Sov. Phys.–Solid State* **29**)